LRP 386/89 October 1989

Invited and Contributed papers
presented at the

14th INTERNATIONAL CONFERENCE ON INFRARED AND MILLIMETER WAVES

Würzburg, F.R.G., October 2-6, 1989

QUASI-OPTICAL GYROTRON:

PRESENT STATUS AND FUTURE PROSPECT

presented by

M.Q. Tran

QUASI-OPTICAL GYROTRON: PRESENT STATUS AND FUTURE PROSPECT

The CRPP/ABB Quasi-Optical Gyrotron Development Group
presented by M.Q. Tran
Centre de Recherche en Physique des Plasmas
Association Euratom-Confédération Suisse
Ecole Polytechnique Fédérale de Lausanne
21 Av. des Bains, 1007 Lausanne, Switzerland

Abstract
A review of the main experiments on quasi-optical gyrotron is presented. Methods to improve the efficiency (pencil beam electron gun and depressed collector) will be discussed.

Introduction
Quasi-optical (Q.O.) gyrotron is an attractive alternative to cylindrical cavity gyrotron at high frequency and high power.With an annular electron beam, theoretical efficiency as high as 30% could be achieved. High power (500kW-1MW) and high frequency (>150GHz) operation was possible [1] while keeping the ohmic heat load on the mirror at about 1-3kW/cm^2. Since the resonator of a Q.O. gyrotron is higly overmoded, tunability can be achieved over a wide range by changing the relativistic electron cyclotron frequency. Finer tuning between two longitudinal modes of the resonator could be achieved by adjusting the mirror resonator. Superconducting (SC) magnet system compatible with the geometry of the Q.O. gyrotron and suitable for operation above 150GHz is within the state of the art of the technology.
Although experiments on Q.O. gyrotron begun only a few years ago, progress has been substantial. In this presentation, we shall review the present status in this field and discuss the various issues related to the enhancement of the Q.O. gyrotron efficiency.

Experimental results
Two main experiments are being performed on Q.O. gyrotron, one at the Naval Research Laboratory (NRL) in Washington, D. C., and the other at our institution. In past experiments, the NRL [2] has achieved power up to 150kW and efficiency up to 12%. The frequency could be tuned between 95 and 130 GHz with only a slight variation in power. The present focus of the NRL group is the test of the Q.O. gyrotron at higher power level using a 4 MW electron beam [3].
The Lausanne experiment experimental setup is described on Fig. 1. The magnetic field is created by a pair of SC magnets in a configuration close to the Helmholtz one. The field profile in the region of the gun is controlled by two SC gun coils.

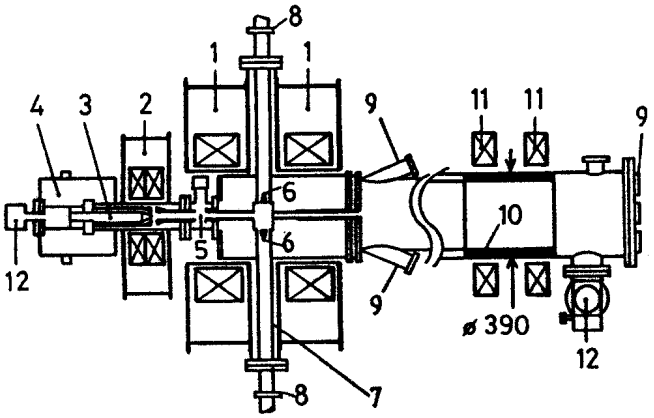

Fig. 1 Experimental setup. The main components are:
1: Main SC coils
2: Gun coils
3: Magnetron injection gun
6: Resonator
8: Mylar window
9: Ports for diagnostics of the electron beam
11:Collector

A large vacuum vessel is inserted inside the room temperature axial and cross bores of the magnet and houses the resonator, the electron beam tunnel and collector. Diagnostics ports are also provided for the measurement of the electron beam properties by electron cyclotron emission [4]. Output power is monitored by a modified Scientec calorimeter and an Octanol one [5]. Time resolved frequency

spectra around 100GHz (fundamental $\omega=\Omega_{ce}$) and 200GHz (second harmonic) are obtained using harmonic ($n=8^+$ at 100GHz, $n=2^+$ at 200GHz) and fundamental (at 100GHz) mixers.
The experiments described in this presentation were performed with a large resonator (Cf. Table I). The microwave energy is extracted from the resonator by diffraction around the edge of both mirrors. The pulse length is limited to 15ms since no cooling is provided to the mirrors or the collector. Power up to 90 kW at 12% RF efficiency was achieved [6] at 100 GHz (Fig. 2) with a 11A beam. Taking into account the coupling and ohmic losses, the electronic efficiency η is estimated to be about 14%. Single mode operation was possible even though the frequency spacing between longitudinal modes is 440MHz.

Beam energy	70keV
Beam current	≤11A
Pulse length	15ms
Designed $p_\perp/p_{//}$	1.5
Optimized $p_\perp/p_{//}$	1.12
Resonator g-parameter	0.338
Mirror separation	33-35cm
Power transmission	4%
Ohmic/Diffractive loss	5%
Coupling efficiency	90%
Beam waist kw_0	31.7

TableI.-Experimental parameters

Spurious emission at the second harmonic occurs while operating the gyrotron with a cavity optimized for fundamental. The second harmonic content was estimated to be about 25% ±10% [7]. A theoretical analysis of the simultaneous excitation of the fundamental and the second harmonic has been performed, which shows that the presence of the fundamental can strongly influence the starting current of the harmonic [8].
Within the operating range of our experimental setup, the frequency could be varied between 98 and 103 GHz (Fig. 3). The power variation is about 10%. Other methods for tuning the frequency (by varying the mirror separation or the beam voltage) were also successfully tested.The output wave, after a propagation length of more than 1m in a cylindrical waveguide (Diameter = 86.4mm), is linearly polarized with the RF electric field $\underline{E}$ perpendicular to the static magnetic field $\underline{B_0}$. The cross - polarization is at least -6dB down. Our program is presently focused on the the generation of second harmonic [7] and the study of the Q.O. gyrotron at high power level (500kW).

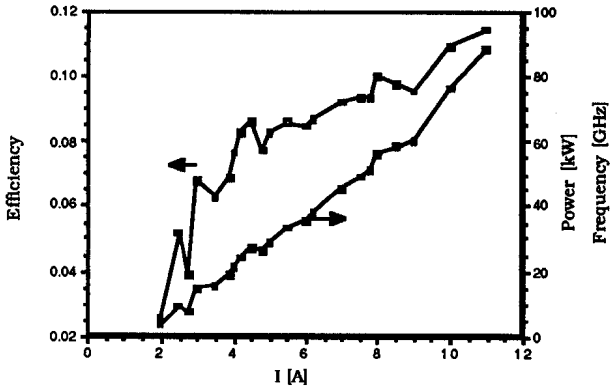

Fig. 2. Variation of the power and efficiency versus beam current I.

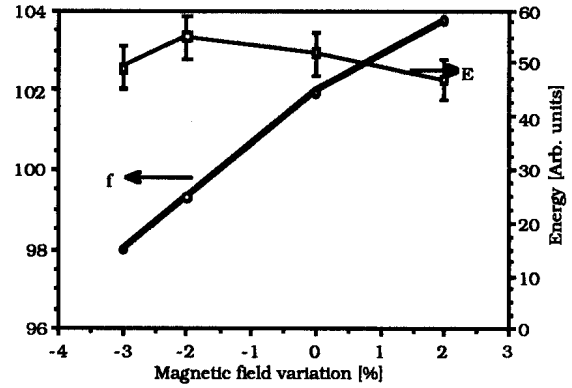

Fig. 3. Tuning range (f) and variation of the output energy E versus $\Delta B_0/B_0$.

Methods for efficiency enhancement

An annular electron beam is not best suited to the geometry of the Q.O. gyrotron, since part of the beam does not interact with the electric field in the resonator. It was shown recently that by tilting the resonator with respect to the $\underline{B_0}$ by $\theta \sim 2/kw_0$, a "pencil beam " efficiency could be obtained using an annular beam [9]. Alternatively, the use of an electron gun delivering pencil beams will also provide an improvement in the efficiency. The key issue in this case is the stability of the beam with respect to electrostatic effect. Recent experiments by Read et al. [10] indicates that such beams can propagate from the gun down to the interaction region (B_0= 4.96T, compression ratio ~ 30) while retaining their geometry. A hot test of such a gun will be performed on one of our Q.O. gyrotrons in the near future.
Implementing a depressed collector is another method to improve the efficiency. A typical distribution function in energy of an 80keV annular beam after the interaction region presents two peaks (Fig. 4). A three stages depressed collector (Fig.5) can have an efficiency (Ratio of the energy recovered in the collector to the energy in the spent beam) as high as 80%, neglecting any detremental

effect due to secondary emission. For the case presented on Figs. 4 and 5, where the electronic efficiency is 0.2 and the collector efficiency 0.75, the total efficiency η of the gyrotron with a depressed collector could be as high as 50%. The design of a depressed collector compatible with the use of a pencil beam still requires development.

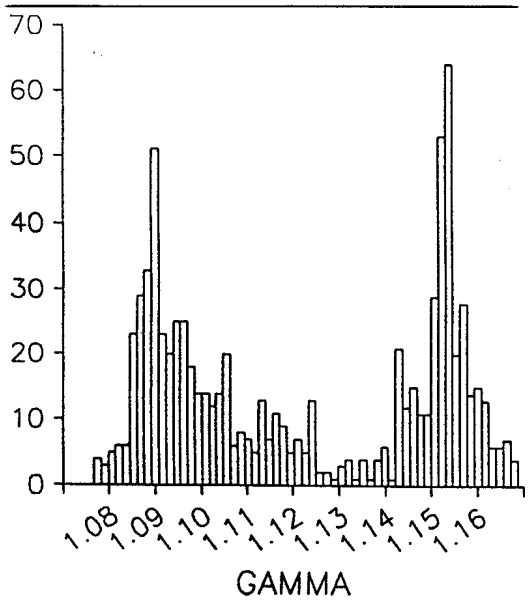

Fig. 4. Distribution function of the electron in the spent beam

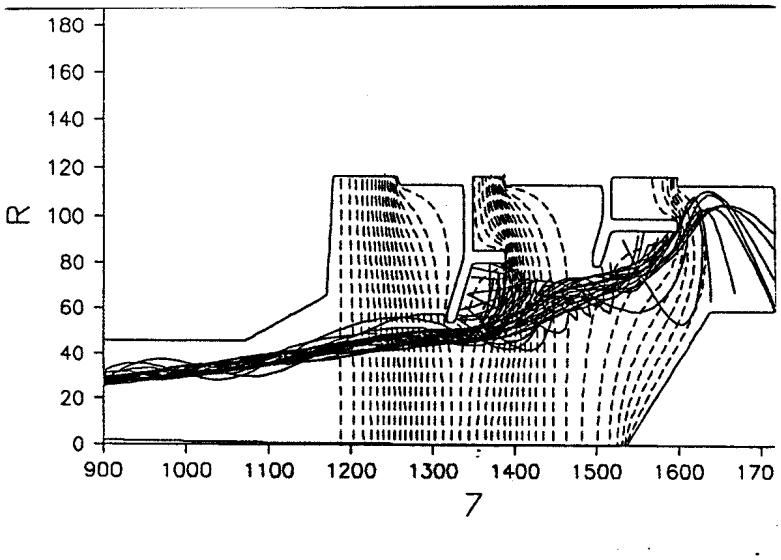

Fig. 5. Schematic of a three stages depressed collector

Conclusion

The proof-of-principle of the Q.O. gyrotron was successfully demonstrated by many experiments. Continuous tunability over a wide frequency domain is also shown. The main issue for this concept lies in its relatively low eficiency η achieved experimentally. However, many methods leading to an enhancement of η exist and are being either implemented or studied. Experiments are now aimed towards high power level in the range of 500kW.

Acknowledgements

This work was partially supported by the Commission pour l'Encouragement de la Recherche Scientifique under grants 1224 and 1564(1224), the Fonds National Suisse pour la Recherche Scientifique under grant 2000-005652 , by NET under contract 330/88-1/FU-CH-NET and by internal R&D funds from the Dept. EKR of ABB-Infocom SA. We would like to acknowledge fruitful discussion and collaboration with Drs. A.W.Fliflet, T. Hargreaves, B. Levush, W. M. Manheimer and M.E. Read.

References

[1] T. M. Tran et al., IEEE Trans. Elect. Dev. **II 36**, 1983 (1989)
[2] A. W. Fliflet et al., Phys. Rev. Lett. **62**, 2664 (1989) and NRL Memorandum report 6459 (1989)
[3] A. W. Fliflet et al., Contributed paper at this Conference
[4] S. Alberti et al., Contributed paper at this Conference
[5] H. Stickel, Int. J. Electronics **64**, 63 (1988)
[6] J. Ph. Hogge et al., Contributed paper at this Conference
[7] S. Alberti et al., Contributed paper at this Conference
[8] T. M. Tran et al., Contributed paper at this Conference
[9] T. Antonsen et al., to be published and Invited paper at this Conference
[10] M. E. Read et al., Contributed paper at this Conference

EXPERIMENTAL STUDY OF A QUASI-OPTICAL GYROTRON

OPERATING

AT THE FUNDAMENTAL FREQUENCY

presented by

J.P. Hogge

EXPERIMENTAL STUDY OF A QUASI-OPTICAL GYROTRON OPERATING AT THE FUNDAMENTAL FREQUENCY

J.P. Hogge, S. Alberti, M.Q. Tran, A. Perrenoud, T.M. Tran, B. Isaak,
A. Bondeson, B. Jödicke* and H.-G. Mathews*
Centre de Recherches en Physique des Plasmas
Association Euratom - Confédération Suisse
Ecole Polytechnique Fédérale de Lausanne
21, Av. des Bains, CH-1007 Lausanne, Switzerland
*Department EKR, ABB Infocom SA, CH-5401 Baden, Switzerland

Abstract
The Centre de Recherches en Physique des Plasmas (CRPP) is developing a 100 GHz ($\omega = \Omega_{ce}$) Quasi-Optical (Q.O) gyrotron. Powers higher than 90 kW at an efficiency of about 12% were recorded [1]. Depending on the electron beam parameters, the frequency spectrum of the output can be either single-moded or multi-moded. One of the main advantage of the Q.O gyrotron is its frequency tunability. We have tested various techniques to tune the output frequency, such as changing the mirror separation, the beam voltage or the main magnetic field. Within the limitations of the present set-up, 5% tunability was achieved.

Experimental set-up
The quasi-optical gyrotron, coils system, resonator and the beam parameters are described in [1], as the power diagnostics. We have two frequency diagnostics for the fundamental ($\omega = \Omega_{ce}$) which allows simultaneous determination of the emission spectrum and study of mode evolution.
The first system provides a fine knowledge of the frequency spectrum and its evolution versus the parameters. It consists of a two stages heterodyne downconvertor system in which the RF signal is fed in a first mixer operating at the 8^{th} harmonic ($f_{RF} = 8f_{LO1} + f_{IF1}$, f_{LO1} swept 11.460 to 11.900 GHz, f_{IF1} in the band 8-12 GHz. The IF1 signal is then amplified, filtered and mixed a second time ($f_{IF1} = f_{LO2} + f_{IF2}$, f_{LO2} = 7.95 GHz, f_{IF2} = 200 MHz. The 200 MHz signal is logarithmically amplified to improve the detection dynamic.
With the second system, the RF is mixed with a 92 GHz Gunn diode signal. The conversion loss of this mixer is much lower than in the first case since it operates at the fundamental. The IF signal is fed in a 16-channel multiplexer, each channel being narrow filtered (center frequency 8-13 GHz, BW 300 MHz). This allows a study of the mode evolution (separation between the modes: 440 MHz). A figure of this set-up can be found in [2], except that the mixer is a $n=1^+$ in our case. Figure 1 is a typical trace obtained through this diagnostic.

Results and discussion
As the electron beam interacts with the standing wave pattern of the cavity, the relative position of the resonator has to be fixed in order to optimize the output power. In agreement with theory [3], a sin(ka) (where a is the displacement and k the wavenumber) modulation of the RF power versus the cavity position has been measured (fig.2). In the single mode theory [4], the emitted frequency ω depends essentially on the detuning parameter 1 - ($\Omega ce/\gamma\omega$) ,where γ is the relativistic factor. Thus, it can be tuned by changing the beam energy (fig.3) or the magnetic field (fig.4). Within the present conditions, a tunability over 5% has been performed without significant change of the power. A fine tuning can be made by changing the mirror separation, as the cyclotron instability bandwidth is much larger than the cavity resonances (fig.5). Finally, as predicted by single mode theory [4], a beam current (I_b) dependence of the frequency has been observed. It is interesting to note that at high current (Ib > 3 A) the dominant mode is out of the instability band (shaded area in fig.6), this might be explained by multimode competition.

Conclusion
The frequency of the quasi-optical gyrotron can be controlled by adjusting the magnetic field, the beam energy, the mirror separation, and the current. The largest tunability (5%) has been achieved by changing the magnetic field. The output power remains almost constant in this domain.
This work was partially supported by Commission pour l'Encouragement à la Recherche Scientifique under grants 1224 and 1564 (1224) and internal R&D fund from ABB Infocom S.A.

References
[1] M.Q. Tran, invited paper at this conference.
[2] S. Alberti et al., contributed paper at this conference.
[3] T.M. Antonsen, B. Levush, W.M. Manheimer, to be published.
[4] A. Bondeson, W.M. Manheimer and E. Ott, in Infr.&MM Waves, K.J. Button ed.,**9**, 309 (1983)

Fig.1

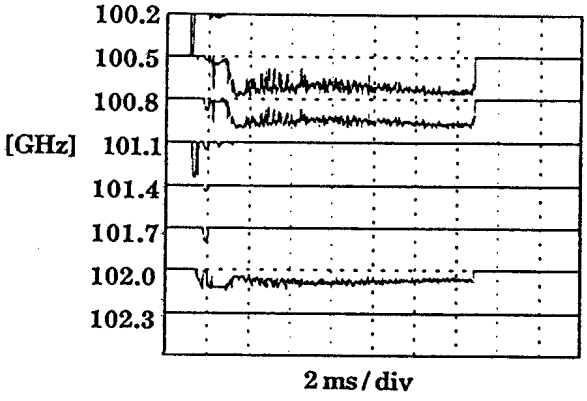

Fig.2

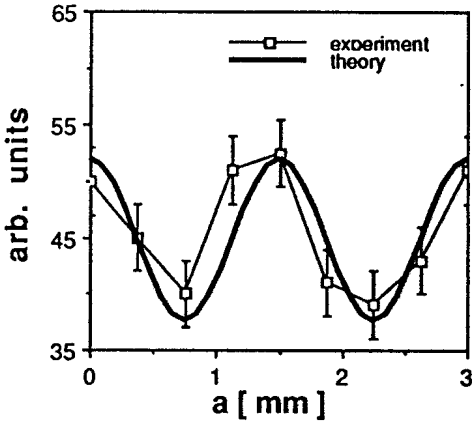

Fig. 3

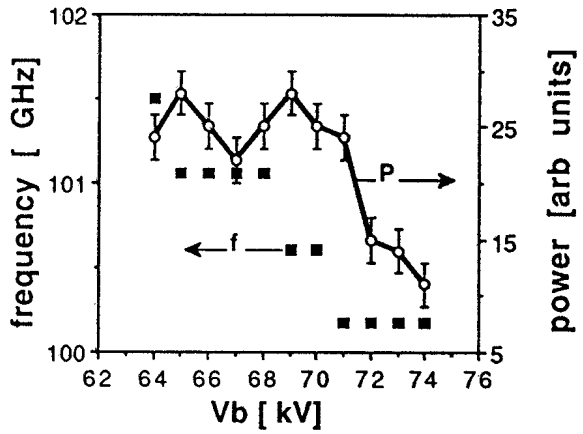

Fig. 4

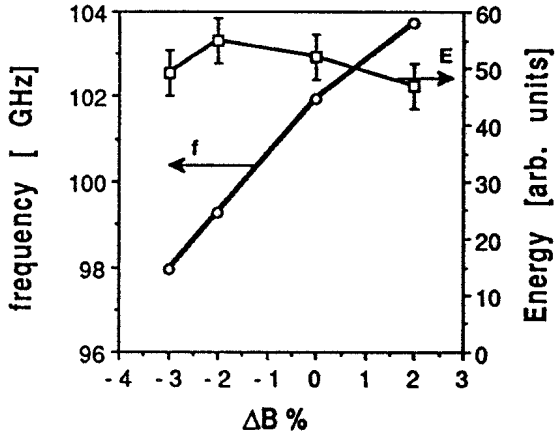

Fig.5

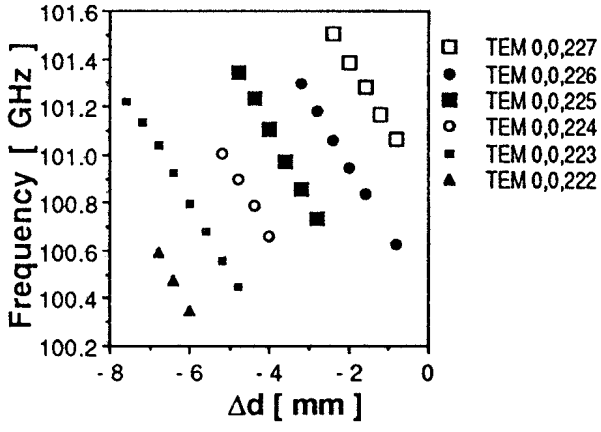

Fig. 6

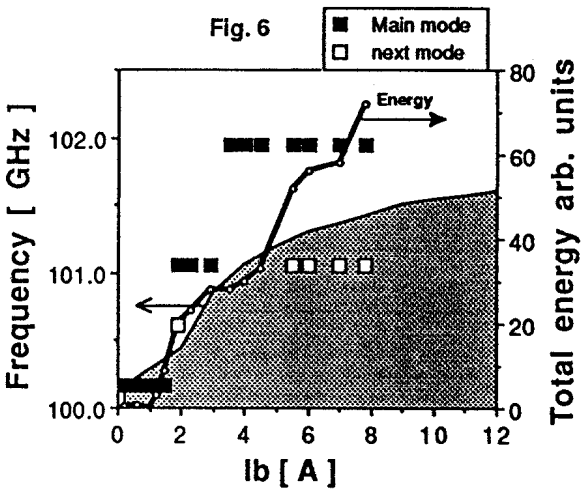

SECOND HARMONIC EMISSION

OF A QUASI-OPTICAL GYROTRON:

EXPERIMENTAL RESULTS

presented by

S. Alberti

SECOND HARMONIC EMISSION OF A QUASI OPTICAL GYROTRON: EXPERIMENTAL RESULTS

S. Alberti, M. Q. Tran, J.P. Hogge, T.M. Tran, A. Bondeson, P. Muggli,
B. Isaak, B. Jödicke*, and H.G. Mathews*
Centre de Recherche en Physique des Plasmas
Association Euratom - Confédération Suisse
Ecole Polytechnique Fédérale de Lausanne
21, Av. des Bains, CH-1007 Lausanne, Switzerland
*Departement EKR, ABB Infocom SA, CH-5401 Baden, Switzerland

Abstract

A quasi-optical (Q.O.) gyrotron designed for operation at the fundamental (Ω_{ce}=100 GHz) exhibits simultaneous emission at Ω_{ce} and $2\Omega_{ce}$. For a beam current of 4A, 20% of the total RF power is emitted at $2\Omega_{ce}$. In order to understand the influence of the presence of the second harmonic on the operation at the fundamental, an extensive set of measurement has been carried out. A comparison with a theoretical model will be presented.

Experiment

The experimental set-up as well as the results concerning the 100 GHz emission are respectively presented in M.Q. Tran et al. in [1] and J.P. Hogge et al. in [2]. The diagnostics for the simultaneous measurement of the 100 GHz and 200 GHz emission are shown in Figure 1. The RF signal is splitted in two part with a mylar foil. The transmitted signal, after -50 dB attenuation through a layer ofOctanol, is down converted to an IF at 8-12 GHz via a 2nd harmonic mixer driven by a Gunn diode operating at 95 GHz. The IF signal is fed into a 16 channel narrow band (300 MHz) multiplexer which allows the analysis of the 2nd harmonic multimode time evolution. The reflected power is collected through a D-band microwave horn and is used for the measurement of the relative power content of the 1st and 2nd harmonic. A 1.32cm thick Macor plate which has a frequency dependent attenuation (μ_i(100 GHz) = 0.75 Np/cm and μ_i(200GHz) = 2 Np/cm) can be placed in front of the detection horn as a verification of this power diagnostic.

Results and discussion

The excitation of the fundamental an the 2nd harmonic versus beam current is shown in Fig.2. One notice mainly two distinct regions of excitation of the 200GHz signal: a first region which goes from the starting current up to 1.1 A exhibits a weak excitation, and the second region which starts around 4A is strongly excited. After introduction of the Macor plate the same measurement as in fig.2 is shown in Fig.3. The comparison of these two figures gives us confidence in this diagnostic.

Figure 4 shows the time evolution of the two modes (100 and 200 GHz). The excited 2nd harmonic Gaussian mode is $TEM_{0,0,2q}$ when the excited fundamental mode is $TEM_{0,0,q}$, this means that the 2nd harmonic frequency is the double of the fundamental. Note the strong competition between the fundamental and the harmonic. When the excitation of the 2nd harmonic is maximum in the first excited region (Ib =1A) no excitation of the fundamental has been observed (Fig. 2 and Fig. 5). The second excited region for the 2nd harmonic (Ib $\geq$ 4A) corresponds to an operation of the Q.O.gyrotron in the hard excitation region for the fundamental frequency.

The presence of the 2nd harmonic while the gyrotron operates in the hard excitation region with respect to the fundamental is in agreement with the theoretical prediction presented by T.M. Tran et al. in [3]. Experiments with a Q.O. cavity designed for operation at the second harmonic only are planned for the near future.

Acknowledgement

This work was partially supported by the Swiss National Science Foundation,
grant no 2000-005651

Reference

[1] M.Q. Tran et al., Invited paper in this conference
[2] J.P. Hogge et al., Contributed paper in this conference
[3] T.M. Tran et al., Contributed paper in this conference

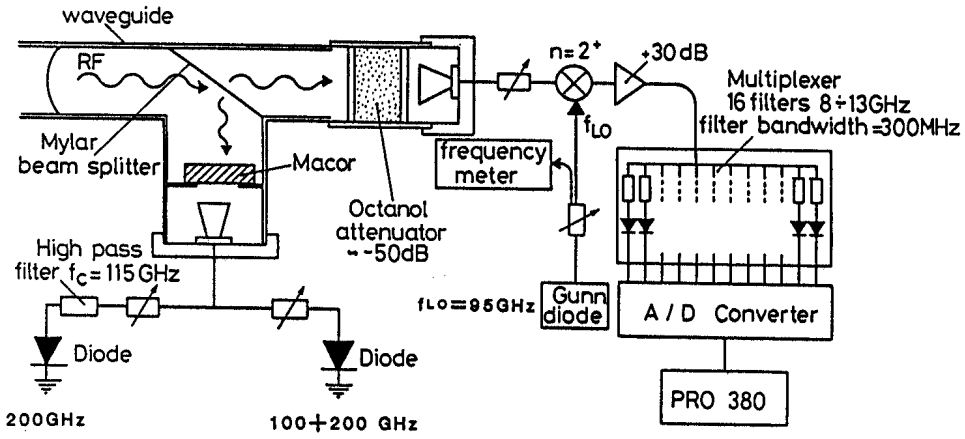

Fig.1

Fig. 2

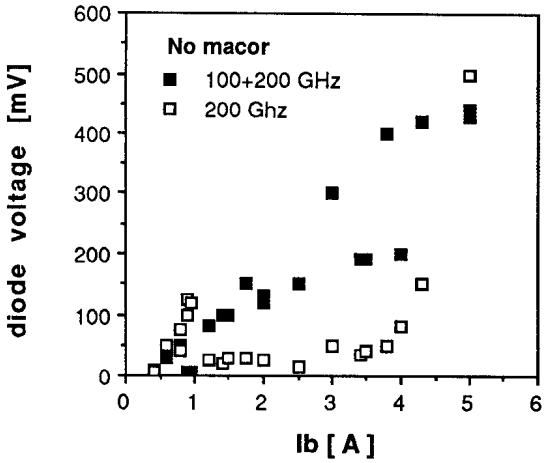

Fig. 3

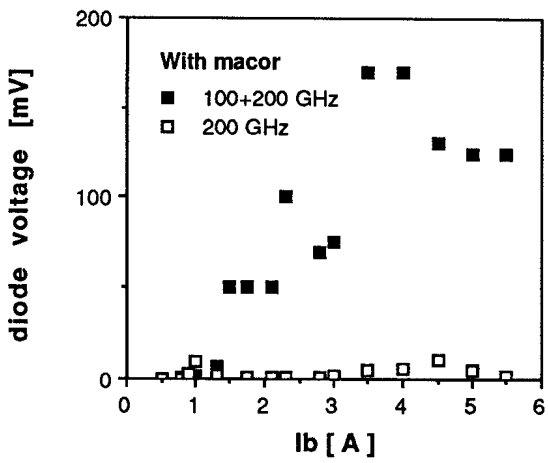

Fig. 4

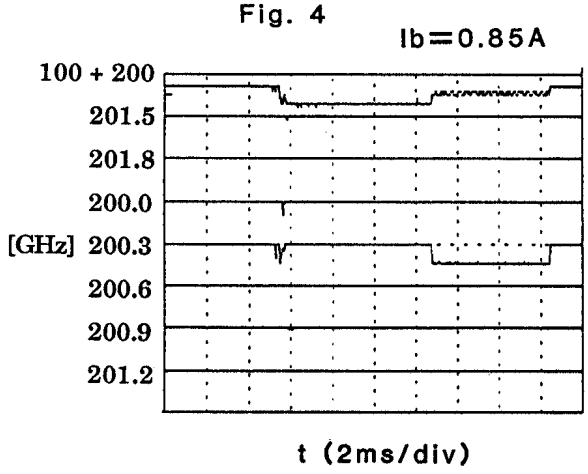

Fig. 5

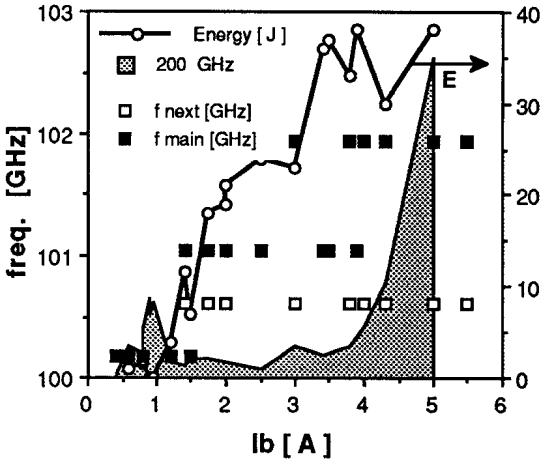

HARMONIC EMISSION IN

QUASI-OPTICAL GYROTRONS

presented by

T.M. Tran

HARMONIC EMISSION IN QUASI-OPTICAL GYROTRONS

T.M. Tran, A. Bondeson, S. Alberti and M.Q. Tran
Centre de Recherche en Physique des Plasmas
Association Euratom - Confédération Suisse
Ecole Polytechnique Fédérale de Lausanne
21, Av. des Bains, CH-1007 Lausanne, Switzerland

Abstract

In a quasi-optical resonator, the quality factor Q is an increasing function of the frequency. As a result, the harmonic content in the output of a high power quasi-optical gyrotron, designed to operate at the fundamental, is expected to be important. Utilizing the slow time scale single particle model, the competition between the fundamental and higher harmonics has been investigated numerically. Small signal as well as nonlinear calculations will be presented. The results can be applied to the design of quasi-optical gyrotrons with high power emission at the second or higher harmonics.

Basic Model

We assume here that the electron beam is a "pencil" beam, interacting with only the Gaussian TEM_{00} modes of the quasi-optical resonator. In addition, we suppose that the different harmonic frequencies satisfy $\omega_n \approx n\omega_1$, with ω_1 denoting the fundamental frequency. Thus the particle slow phase θ_n is related to its fast phase ψ and the electric field phase ϕ_n by

$$\theta_n = n\psi - (\omega_n t + \phi_n) = n\theta_1 - \phi_n \tag{1}$$

where we assume that $\phi_1 = 0$. Using then the normalized variables introduced in [1,2], the slow time scale particle equations can be expressed as

$$\frac{dp}{d\zeta} = -i(\Delta - 1 + |p|^2)p - \sum_n n F_n e^{i\phi_n} (p^*)^{n-1} f_n(\zeta) \tag{2}$$

where $p = (\gamma\beta_\perp / \gamma\beta_{\perp 0}) \exp(i\theta)$ is the particle complex transverse momentum and Δ is the normalized detuning parameter. The electric field, at the nth harmonic is characterized by its amplitude F_n, phase ϕ_n and axial profile f_n which is taken as a Gaussian:

$$f_n(\zeta) = e^{-\left(2\zeta/\mu_n\right)^2} \tag{3}$$

where μ_n is the normalized interaction length. The Eq.(2) is a straightforward extension of the single mode equation derived in [3]. The wave amplitude can be determined by the following wave equation, expressed with the dimensionless time $\tau = \omega_1 t / 2Q_1$ (see ref.[4]):

$$\frac{dF_n}{d\tau} = n\frac{Q_1}{Q_n} F_n (\chi_n I_n - 1) \tag{4}$$

where I_n is the normalized current and Q_n is the resonator quality factor for the frequency ω_n. The gain function χ_n is defined by

$$\chi_n(F_1, F_2, \cdots, \phi_1, \phi_2, \cdots) = 2\,Re\left[\frac{n}{F_n e^{i\phi_n}} \int_{-\infty}^{+\infty} d\zeta \langle p^n \rangle f_n(\zeta)\right] \tag{5}$$

Because of the equidistant frequency spectrum, we can assume that the phase ϕ_n of the nth harmonic field component seen by the particles is uniformly distributed over the interval $[0, 2\pi]$ so that one can average Eq.(5) over ϕ_n. Thus the particle equation (2) together with the wave equation (4) determine completely the multimode excitation of the quasi-optical gyrotron. In the steady state, the operating conditions can be obtained from the following balance equations:

$$\chi_n(F_1, F_2, \cdots) = 1/I_n \tag{6}$$

which relate the field amplitude at each harmonic to the electron beam current and resonator loss.

Starting Conditions

The starting conditions can be analyzed by using the multimode equations (2) and (4) presented above. Let consider the case in which only the fundamental (n=1) and the second harmonic (n=2) field components are present in the system. The fundamental mode stability can be studied by setting

$$\begin{aligned} F_1 &= F_{10} + \delta F_1 \\ F_2 &= 0 \quad + \delta F_2 \end{aligned} \tag{7}$$

where δF_1 and δF_2 are small perturbations around the steady state amplitudes $F_{10} \neq 0$ and $F_{20} = 0$. Inserting the expressions (7) into the wave equation (4) and keeping only the first order terms (in δF_1, δF_2), a criteria for the instability of the fundamental (or excitation of the second harmonic) can be obtained. Furthermore, since $F_{20} \rightarrow 0$, a linearization [4] in F_{20} can be done on the particle equation (2), yielding a computationally simpler set of equations. In Fig.(1), we show a result obtained numerically, using such an approach. One can observe that the strong fundamental interaction can decrease the second harmonic linear gain χ_2 (which is inversely proportional to the starting current). However, in the hard-excitation region of the fundamental operation, this gain increases rapidly from its single mode value $\chi_2 (F_2 = 0) = 28.2$. Notice that the same method can be applied to study the stability of operation at any harmonic number n against another parasitic mode m. The procedure becomes however cumbersome when an arbitrary number of harmonics are simultaneously taken into account.

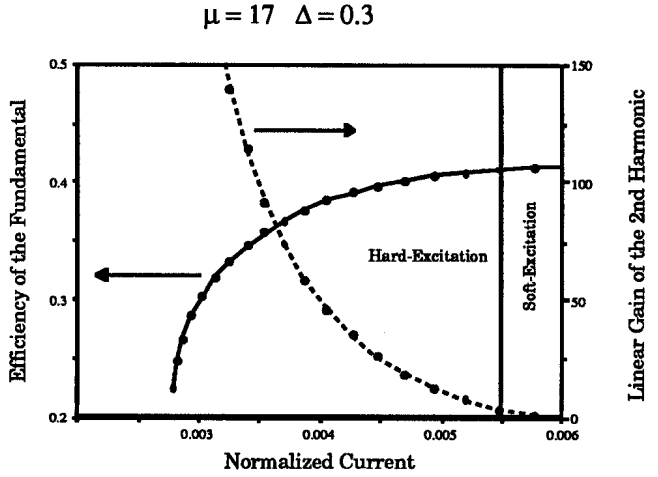

Figure 1. Nonlinear efficiency of the fundamental and the linear gain of the second harmonic versus the normalized current

Conclusions

From a multimode formulation of the slow time scale equations, we have applied a simple method to analyze the mode stability of a quasi-optical gyrotron in which both the fundamental and the second harmonic modes can coexist. Such calculations are useful for the experiment interpretation as well as for the design of high frequency devices. This method has been extended to determine the non-linear efficiencies in a quasi-optical in which several harmonics may be excited simultaneously.

References

[1] V.A. Flyagin, A.L. Goldenberg and N.S. Nusinovich, "Powerful gyrotrons", in Infrared and Millimeter Waves, K.J. Button, ed. 1984, p.179

[2] B.G. Danly and R.J. Temkin, Phys. Fluids, 29 (1986) 1274.

[3] A. Bondeson, W.M. Manheimer and E. Ott, "Multimode analysis of quasi-optical gyrotrons and gyroklystrons", in Infrared and Millimeter Waves, K.J. Button, ed. 1983, p.309

[4] G.S. Nusinovich, Int. J. Electronics, 51 (1981) 457

A NOVEL ELECTRON BEAM DIAGNOSTIC

USING THE MEASUREMENT OF

THE CYCLOTRON EMISSION (ECE)

presented by

S. Alberti

A NOVEL ELECTRON BEAM DIAGNOSTIC USING THE MEASUREMENT OF THE CYCLOTRON EMISSION (ECE)

S. Alberti, M.Q. Tran. , T.M. Tran, J. P. Hogge, P. Muggli, B. Isaak
Centre de Recherche en Physique des Plasmas
Association Euratom - Confédération Suisse
Ecole Polytechnique Fédérale de Lausanne
21, Av. des Bains, CH-1007 Lausanne, Switzerland

Abstract

A new method for the measurement of the parallel momentum distribution function of a monoenergetic magnetized weakly relativistic electron beam is presented. A gyrating electron having a parallel velocity $\beta_{//}$ emits a radiation at a doppler shifted frequency given by $\omega = \omega_0(1 - \beta_{//} \cos\theta)^{-1}$ where θ is th observation angle and ω_0=qB/m. Therefore, at a given θ , the measurement of the emitted spectrum of an electron beam gives, in a straightforward manner, the distribution function in $\beta_{//}$. In our analysis we take into account relativistic effects on the angular distribution of the emission as well as the experimental constraints such as the angular dependency of the gain of the antenna used for the detection. Experimental results will be presented for a 70 keV annular electron beam.

Theoretical model

A weakly relativistic treatment of the theory of the cyclotron emission of an electron in a static magnetic field will be presented, therefore only the emission at the fundamental frequency will be considered.

Taking account of this assumption the total power $\eta(\omega,\Omega)$ emitted per unit solid angle per frequency interval $d\omega$ is given by[1] :

$$\eta\left(\omega,\beta_{//},\beta_{\perp},\theta\right) = \frac{e^2}{32\pi^2\varepsilon_0 c}\left(\frac{\omega_0}{\gamma}\right)^2 \frac{1}{\left(1-\beta_{//}\cos\theta\right)^2}\beta_{\perp}^2\left[\left(\frac{\cos\theta-\beta_{//}}{1-\beta_{//}\cos\theta}\right)^2+1\right]\delta(w) \qquad [1]$$

where $w=\omega_0 - \omega(1-\beta_{//}\cos\theta)$ and a first order developement of the Bessel function is taken.The angular distribution of the total power is shown in Fig.1.Integrating [1] over the normalized parallel distribution function:

$$f\left(\beta_{//}\right) = N\exp\left[-\left(\frac{m_0\gamma c^2}{2k_B T_{//}}\right)\left(\beta_{//}-\beta_{//_0}\right)^2\right] \qquad [2]$$

and replacing $\beta_{\perp}=[1-\beta_{//}^2-(\gamma^2)^{-1}]^{1/2}$ (monoenergtic beam) one obtains the emitted power density [W/(m^3 Hz srad)]:

$$\left(\frac{d^3P}{d\omega\, dV\, d\Omega}\right)d\omega = n_0 f\left(\beta_{//}\right)\eta\left(\beta_{//},\theta\right)\frac{1}{\left(1-\beta_{//}\cos\theta\right)}d\beta_{//} \qquad [3]$$

For a given observation angle θ [3] gives the frequency spectrum of the emitted power by a beam element (Fig.2 a).Finally integrating [3] over the velocity space (equivalent to an integration over the frequency) from β_{min} to β_{max} one gets the emitted power density per unit volume and solid angle.

Experimental setup and results

The experimental setup is shown in Fig.3. A conventional heterodyne detection is used for the measurement of the frequency spectrum of the emitted power.The radiated power is collected through a rectangular D-band microwave horn, therefore only the y-polarisation of the emitted electric field is measured. Eq. [1] considers the power emitted in all polarisation, the equivalent of Fig.1 but only for the angular distribution for the y-polarisation is shown in Fig.4.The total power collected by the microwave horn is then obtained after integration of eq. [3] over the beam volume seen by the antenna and taking account of the antenna gain.The integration limits over the velocity space are such that all the experimental constraints are satisfied. Fig.2 shows the comparison between the spectrum emitted by a beam element (continuous line) and the spectrum measured for a typical experimental simulation (dots), note that for the choosen observation angle the line width corresponding to the beam temperature is the same in both cases. For a typical experimental condition (see Fig.4) the collected power is of the order of -25dBm (5 μW) which is above the threshold of -50dBm of the heterodyne detection. A typical experimental spectrum is shown in Fig. 5. This measurement was performed in the presence of the gyrotron interaction which can highly perturb the

parallel distribution function (creation of different energy population in the electron beam), but this preliminary results shows the powerfulness of the diagnostic.

Reference

[1]G. Bekefi, *in Radiation processes in plasmas,* J. Wiley and sons, editor, Chap. 6 (177), (1966)

Fig. 1

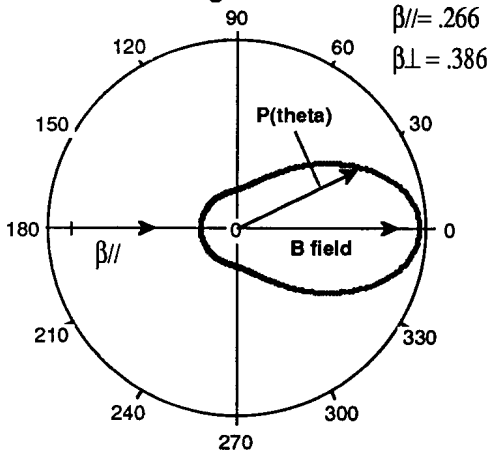

Fig. 2

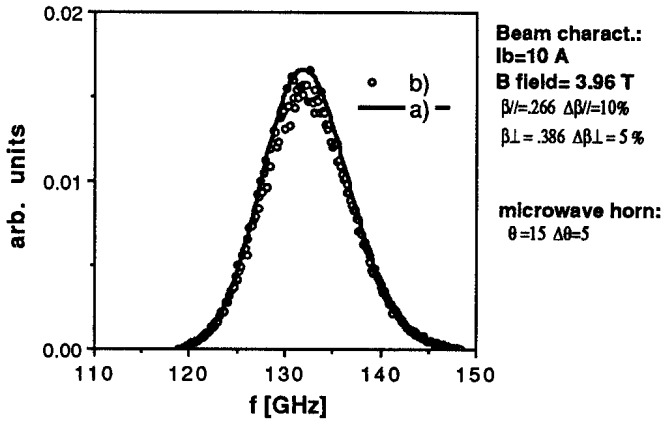

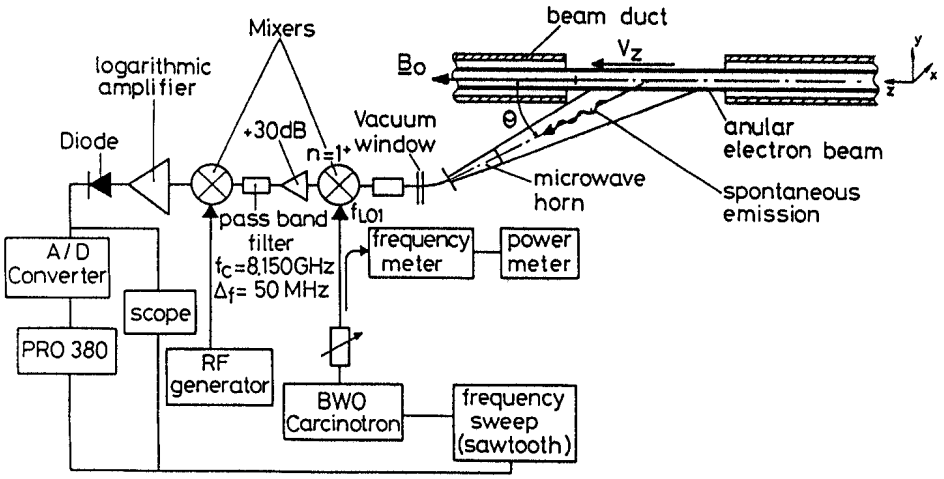

FIG. 3

Fig. 4

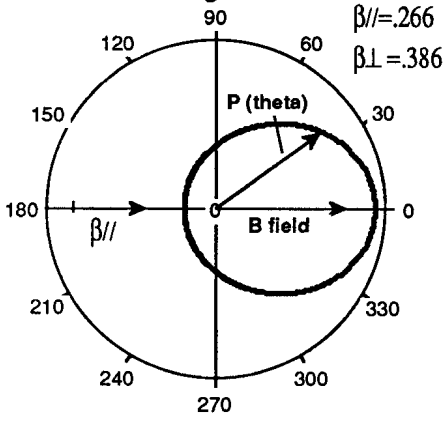

Fig.5

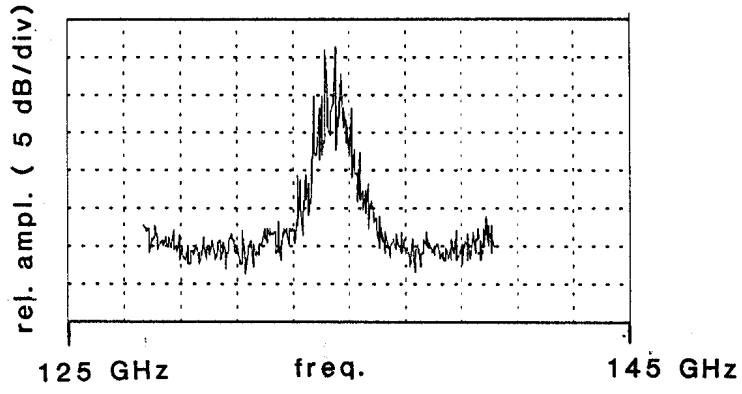

LOW POWER MEASUREMENT OF POWER COUPLING OUT OF FABRY-PEROT RESONATOR AT mm WAVELENGTHS. COMPARISON BETWEEN SOME TECHNIQUES.

presented by

J.P. Hogge

LOW POWER MEASUREMENT OF POWER COUPLING OUT OF FABRY-PEROT RESONATOR AT mm WAVELENGTHS. COMPARISON BETWEEN SOME TECHNIQUES.

J.-P. Hogge, A. Perrenoud, M.Q. Tran, S. Alberti, B. Isaak, P. Muggli and T.M. Tran
Centre de Recherches en Physique des Plasmas
Association Euratom - Confédération Suisse
Ecole Polytechnique Fédérale de Lausanne
21, Av. des Bains, CH-1007 Lausanne, Switzerland

Abstract
Three different ways of coupling energy out of a large Fabry-Perot resonator have been tested at frequencies around 120 GHz, in the frame of quasi-optical gyrotron developement. Coupling through annular slots in one of the mirrors, Cassegrain coupling and power extraction through a mirror perforated with parallel slits acting as a strip grating have been compared after propagation in a strongly overmoded circular waveguide by measuring the field pattern at different positions.

Theoretical considerations
With the use of a slotted mirror (fig. 1a) or a Cassegrain system (fig. 1b), the coupling is purely diffractive whereas in the third case (fig. 1c) the mirror can be considered as semi-transparent.
Marcuvitz [1, eq.2a p.218] has given a formula for the transmission coefficient of infinitely thin capacitive strip gratings, valid for the case $a/\lambda < 1$, and electric field perpendicular to the strips. The slits can be considered as waveguides propagating TE_{no} modes.The measure of the radiated field does not allow to know directly the mode of propagation inside the tube but it provides a good idea of it.

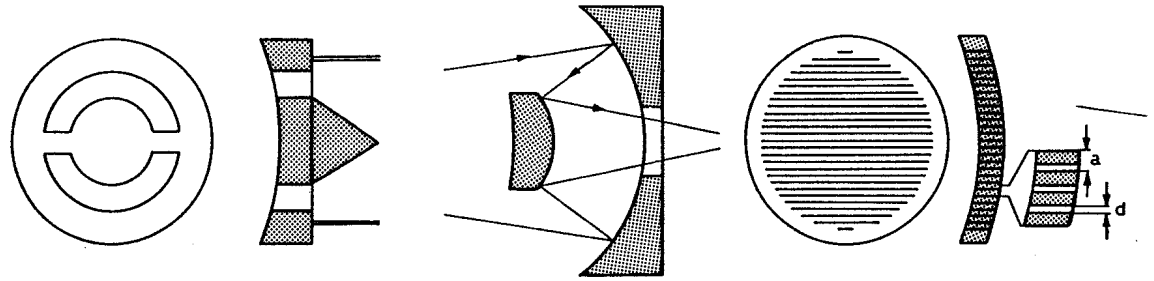

Fig.1a Fig.1b Fig.1c

Experimental set-up

A grid mirror has been manufactured with a/λ=1.09, a/d=2.9, giving a transparency of a few percents. The experimental test stand is shown on fig. 2. The source is a carcinotron. The cavity consists of one spherical metal mirror and the test mirror separated by 50 cm. It is fed by a D-band rectangular open wave guide which excites TEM_{00q} (q~400) gaussian mode. The overmoded waveguide is a 150 mm diameter and 4m length copper tube ($\varnothing = 60\,\lambda$) . The RF field is detected by a harmonic mixer ($f_{RF} = n\,f_{LO} + f_{IF}$, n=12, f_{LO} = 10GHz, f_{IF} = 200 MHz) and the IF signal is put in a logarithmic amplifier, thus giving the result in dB. The mixer is placed on an XY arm allowing scans over a 10 x10 cm region.

Results and discussion
Bidimensional scans have been performed with the three configurations, at 10-20 cm and at 50cm of the tube. Plots showing equal power lines are presented. On each plot, the regions corresponding to power ≤-8db below the maximum have been neglected for clarity. The separation between each contour is always 1 dB. Although the amplitude of the maxima is almost the same for each coupling configuration, a comparison would require a careful calibration of the complete system (the conversion loss of the mixer depends sensitively on the frequency and LO power and is therefore difficult to estimate since the system is each time set to have the maximum dynamic). Figs. 3a and 3b correspond to the Cassegrain antenna, taken respectively at 20 and 50 cm of the end of the tube. At 20 cm, a central structure surrounded by secondary lobes appears, but there is no real dominant peak. At 50 cm, a peak is observed, with 3 islands at -6dB each. A possible explanation of this 4-peak structure is a slight misalignment of one of the mirrors, the system being very sensitive to alignment. Figs. 4a and 4b correspond to the slotted mirror, measured 10 and 50 cm from the tube. A strong central peak is observed at 10 cm, but this structure is not conserved: at 50 cm the center is a minimum. The grid mirror (figs. 5a and 5b) gives a narrow central peak at 10 cm, but with a -5 dB island. From the

three coupling schemes, it exhibits the best field pattern at 50 cm. It should be noted that - at the difference of the two other mirrors - the central peak structure exists along all the path, at least up to 50 cm from the tube.

In each case, there seems to be a kind of focalisation at ~ 10 cm of the tube. This is interpreted as being the effect of the tube itself.

Conclusion

From the three tested coupling schemes, the most promising for gyrotron applications seems to be coupling by the grid mirror since it has a radiation pattern which looks at most beamlike. Nevertheless, some problems as cooling of the mirror will become sharp when hot tested, this problem might be solved more easyly with slotted mirrors or Cassegrain coupling.

We would like to thank Dr. L. Rebuffi for helpful discussions.

Reference

[1] N.Marcuvitz, *Waveguide Handbook, M.I.T Radiation Laboratory Series,* McGraw-Hill (1951)

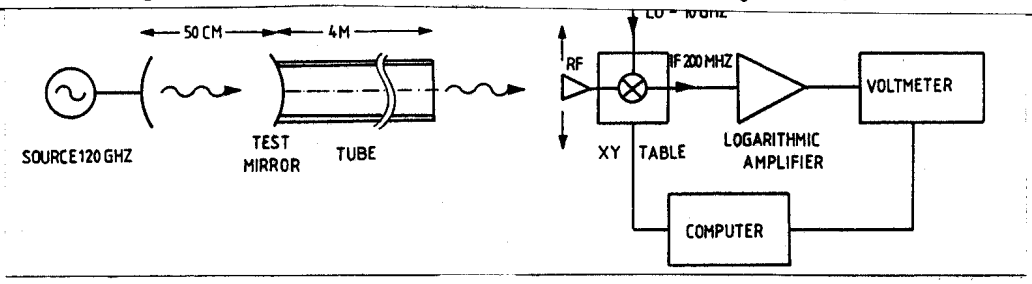

Fig.2

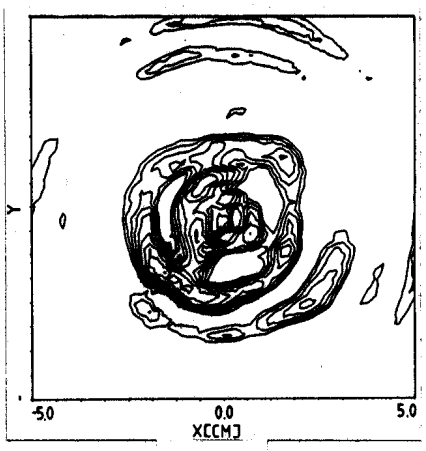

Fig. 3a

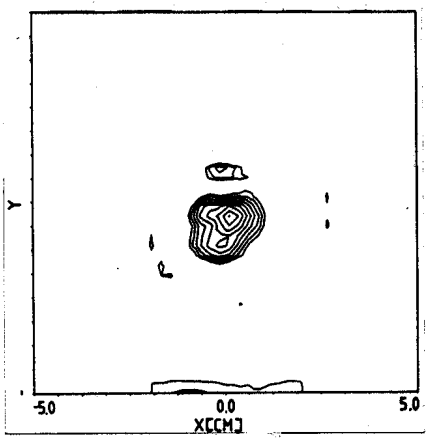

Fig.4a

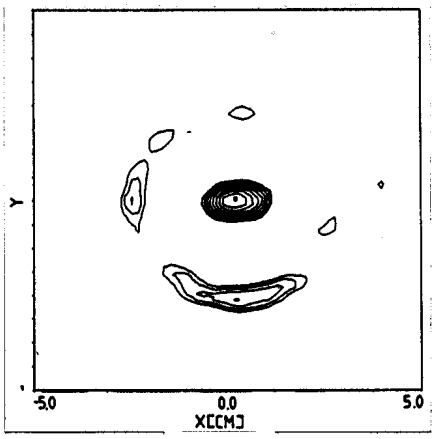

Fig.5a

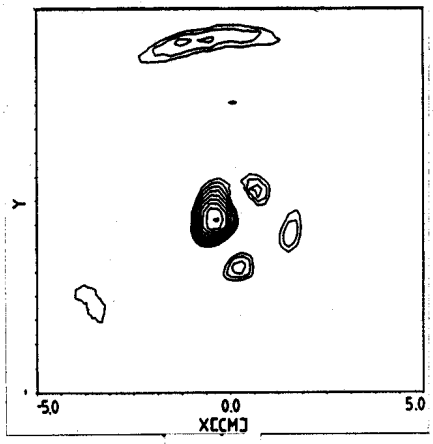

Fig.3b

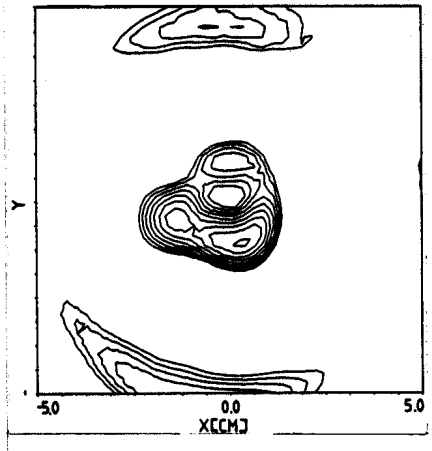

Fig.4b

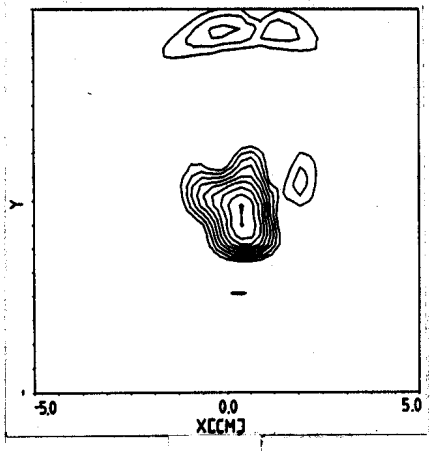

Fig.5b

MULTIMODE SIMULATION OF

FREE-ELECTRON-LASER OSCILLATORS

presented by

T.M. Tran

MULTIMODE SIMULATION OF FREE-ELECTRON-LASER OSCILLATORS

T.M. Tran and D. Dietrich
Centre de Recherche en Physique des Plasmas
Association Euratom - Confédération Suisse
Ecole Polytechnique Fédérale de Lausanne
21, Av. des Bains, CH-1007 Lausanne, Switzerland

Abstract
The nonlinear evolution of a free-electron-laser (FEL) oscillator is investigated numerically for a configuration in which the FEL gain per pass in a high Q optical resonator is low. In this configuration, the number of passes required to reach the nonlinear saturation can be very large. In order to reduce the computer time, a formulation in which the discrete pass number is transformed to a continuous slow time variable is used. Preliminary results will be presented for the case where the 2-D effects (diffraction, betatron oscillations) are neglected.

Physical Model
We assume here a 1D model for the FEL, neglecting thus the particle betatron motion as well as the radiation diffraction. Taking into account the time dependant effects, the 1D trajectory of an electron labelled by $j = 1,\cdots,N_p$ is characterized by its energy $\gamma_j(z)$, phase angle $\theta_j(z)$, and "retarded time" $t'_j(z) = t_j(z) - z/c$, which are governed by the following ODEs:

$$\frac{d\gamma_j}{dz} = -\frac{\omega_s}{\gamma_j c} a_w a_s^{(n)} \sin\left(\theta_j + \phi_s^{(n)}\right) \tag{1.a}$$

$$\frac{d\theta_j}{dz} = k_w - \frac{\omega_s}{c}\frac{1 + a_w^2 - 2a_w a_s^{(n)} \cos\left(\theta_j + \phi_s^{(n)}\right)}{2\gamma_j^2} \tag{1.b}$$

$$\frac{d(ct'_j)}{dz} = 1/\beta_z - 1 = \frac{1 + a_w^2 - 2\,a_w a_s^{(n)} \cos\left(\theta_j + \phi_s^{(n)}\right)}{2\,\gamma_j^2} \tag{1.c}$$

During pass n through the resonator, the radiation field, denoted by its complex amplitude

$$\mathcal{A}^n(t',z) = a_s^{(n)}(t',z)\exp\left[i\phi_s^{(n)}(t',z)\right]$$

is assumed to be constant in z, as one can expect in a low gain FEL oscillator (or in the near-saturation regime). Furthermore, when the resonator diffraction loss is small (high Q resonator), one can replace the discrete pass number n by a continuous slow time $\tau = nT_r$, T_r being the radiation round-trip time in the resonator [1], and obtain the following PDE for the radiation field:

$$\left[\frac{\partial}{\partial\tau} + \frac{\omega_s}{2Q}\right]\mathcal{A}(t',\tau) = \frac{i}{2k_s T_r}\frac{eZ_0}{mc^2}\frac{Q_b}{A_b N_p}\int_0^L dz \sum_{j=1}^{N_p} \delta(t'-t'_j)\frac{a_w e^{-i\theta_j}}{\gamma_j} \tag{2}$$

together with the periodic boundary condition:

$$\mathcal{A}(t'+T_r,\tau) = \mathcal{A}(t',\tau) \tag{3}$$

In writing Eq.(2), we have assumed that each of the simulation electron carries a charge $Q_b/A_b N_p$, where Q_b and A_b are the total charge and the cross-section of the electron pulse injected into the wiggler, respectively.

Simulation Model
The t' discretization is done by considering a grid on the t' axis on which are defined the grid values $\mathcal{A}_k(\tau) = \mathcal{A}(t'_k,\tau)$. Integrating Eq.(2) on each of the intervals $[t'_{k-1/2}, t'_{k+1/2}]$ transforms then the PDE (2) into the system of ODEs for $\mathcal{A}_k(\tau)$:

$$\Delta t'_k \left[\frac{d}{d\tau} + \frac{\omega_s}{2Q}\right] \mathcal{A}_k(\tau) = \frac{i}{2k_s T_r} \frac{eZ_0}{mc^2} \frac{Q_b}{A_b N_p} \int_0^L dz \sum_{j \in \mathcal{J}_k} \frac{a_w e^{-i\theta_j}}{\gamma_j} \qquad (4)$$

where $\mathcal{J}_k$ denotes the particles that are located inside the interval $[t'_{k-1/2}, t'_{k+1/2}]$. In the particle equations (1), the radiation field $\mathcal{A}(t'_j, \tau)$ seen by the particle j is approximated by the value of $\mathcal{A}_k(\tau)$ at the grid point that is the nearest the value of t'_j. This field interpolation, together with the particle charge assignment as prescribed in the RHS of Eq.(4), is analogous to the so-called "nearest-grid-point" or NGP scheme employed in particle simulation of plasmas.

The time stepping (in τ) is done, using the explicit scheme that can be outlined as follow:

(a) Advance the field from τ to $\tau + \Delta\tau$, assuming that the source term in Eq.(4) is known at τ. (b) Advance the particles by integrating Eqs.(1), using a low storage fourth order Runge-Kutta algorithm [2], from the entrance of the wiggler $z = 0$ to the exit of the wiggler $z = L$. The field seen by the particles is interpolated from the updated grid values $\mathcal{A}_k(\tau + \Delta\tau)$. (c) Construct finally the updated source term as prescribed in the RHS of Eq.(4). The next time step, starting from step (a) can now be performed.

The implementation of the procedure presented above has been done and optimized for the Cray-2. The CPU time used is typically 0.33 ms per particle and per time step, for a run in which the number of grid points on the t' axis is 64 and 500 points are taken for the Runge-Kutta integration in z.

One drawback of this explicit time stepping is that it requires a rather small time step $\Delta\tau$. In cases where mode competition is strong, the number of steps required to reach the saturation may be prohibitive (several hundreds). We are experimenting iterative implicit time stepping schemes which can allow much larger time steps. These schemes are expected to reduce drastically the overall CPU time, so that a full FEL simulation in which 2D or 3D effects such as the radiation diffraction and the particle transverse motion (betatron oscillation) are included, becomes more tractable.

Acknowledgement

This work was supported by the Swiss National Science Foundation, grant No 2000-005651.

References

[1] N.S. Ginzburg and M.I. Petelin, Int. J. Electron. 59 (1985) 291.

[2] E.K. Blum, Math. Comp., 16 (1969) 176.